

# Animal Model

## Cryoglobulinemic Glomerulonephritis in Thymic Stromal Lymphopoietin Transgenic Mice

Sekiko Taneda,\* Stephan Segerer,\*  
Kelly L. Hudkins,\* Yan Cui,\* Min Wen,\*  
Manuela Segerer,\* Mark H. Wener,<sup>†</sup>  
Christian G. Khairallah,<sup>‡</sup> Andrew G. Farr,<sup>‡</sup> and  
Charles E. Alpers\*

From the Departments of Pathology,\* Laboratory Medicine,<sup>†</sup> and  
Biological Structure,<sup>‡</sup> University of Washington,  
Seattle, Washington

**Mixed cryoglobulins are complexes of immunoglobulins that reversibly precipitate in the cold and lead to a systemic disease in humans. Renal involvement usually manifests as a membranoproliferative glomerulonephritis with marked monocyte infiltration and, at times, intracapillary thrombi. Thymic stromal lymphopoietin (TSLP) is a recently cloned cytokine that supports differentiation and long-term growth of B cells. Here we report that TSLP overexpression in mice results in the development of mixed cryoglobulins, with renal involvement closely resembling cryoglobulinemic glomerulonephritis as it occurs in humans. One hundred twenty-three mice were sacrificed at monthly intervals, with at least five TSLP transgenic mice and five controls in each group. Blood, kidneys, spleen, liver, lung, and ear were collected and studied by routine microscopy, immunofluorescence, immunohistochemistry, and electron microscopy. TSLP transgenic animals developed polyclonal mixed cryoglobulinemia (type III) and a systemic inflammatory disease involving the kidney, spleen, liver, lung, and ears. Renal involvement was of a membranoproliferative type demonstrating thickened capillary walls with cellular interposition and double contours of the basement membrane, expansion of the mesangium because of increased matrix and accumulation of immune-deposits, subendothelial immune-deposits, focal occlusion of capillary loops, and monocyte/macrophage influx. In contrast to the severe glomerular lesions, the tubulointerstitium was not involved in the disease process. The renal lesions and the disease course were more severe in females when compared to males. We describe a mouse strain in which a B-cell-promoting cytokine**

**leads to formation of large amounts of mixed cryoglobulins and a systemic inflammatory injury that resembles important aspects of human cryoglobulinemia. This is the first reproducible mouse model of renal involvement in mixed cryoglobulinemia, which enables detailed studies of a membranoproliferative pattern of glomerular injury. (Am J Pathol 2001, 159:2355–2369)**

Immunoglobulins (Igs) or complexes of Igs that reversibly precipitate *in vitro* at low temperatures are called cryoglobulins.<sup>1–6</sup> According to the components of the cryoprecipitates, cryoglobulins are currently divided into three groups.<sup>7</sup> Type I cryoglobulins consist of a monoclonal Ig or light chain and are usually associated with lymphoproliferative disorders. More common are mixed cryoglobulins, which are complexes of two or more Igs, in which IgG is bound by an Ig with anti-IgG (rheumatoid factor) activity.<sup>7–9</sup> The anti-globulin component is monoclonal in type II cryoglobulins, whereas type III cryoglobulins contain more than one polyclonal Ig class.<sup>7</sup> Typical diseases associated with mixed cryoglobulins are infections (eg, hepatitis C virus) and autoimmune diseases.<sup>7,10</sup> It has been estimated by the World Health Organization that 3% of the world's population, are infected with hepatitis C virus (Weekly Epidemiological Record. N°49, 10 December 1999, World Health Organization). Although liver disease is the principal consequence of such an infection, hepatitis C virus also results in extra-hepatic manifestations including mixed cryoglobulinemia and membranoproliferative glomerulonephritis (MPGN).<sup>11</sup> Although the percentage of hepatitis C virus-infected patients with such manifestations is small, the problem is significant as the population at risk is so large.

Supported in part by grants from the KIDNEEDS foundation, the Northwest Kidney Centers Foundation, pilot project funds from the National Institutes of Health (grant U19 AI41320 and grant A144160), and a grant from the Else Kröner-Fresenius-Stiftung, Bad Homburg v. d. Höhe, Germany.

S. T. and S. S. both contributed equally to this work.

Accepted for publication August 27, 2001.

Address reprint requests to Dr. Charles E. Alpers, University of Washington Medical Center, Department of Pathology, Box 356100, Seattle, WA 98195. E-mail: calp@u.washington.edu.

Indeed, it is now regarded that hepatitis C virus is associated with the great majority of cases of what had been previously thought to be idiopathic MPGN and essential mixed cryoglobulinemia.

Clinical manifestations of cryoglobulinemia can include involvement of the skin, kidney, central nervous system, gut, vascular system, and the lung.<sup>6</sup> The typical renal manifestation is a membranoproliferative pattern of glomerulonephritis with periodic acid-Schiff (PAS)-positive deposits (containing the cryoglobulins in immune complexes) filling capillary lumina (hyaline thrombi), endocapillary proliferation with prominent infiltration of capillaries by monocyte/macrophages, and, at times, vasculitis involving small- and medium-sized renal arteries.<sup>12,13</sup> The pathogenesis of this important form of glomerulonephritis is still incompletely understood. In part this has been because of the lack of a reliable animal model of this disease process.

Thymic stromal lymphopoietin (TSLP) has been isolated from conditioned medium of a thymic stromal cell line and supports differentiation of IgM-positive B cells.<sup>14,15</sup> This 140-amino acid protein supports the growth of pre-B cell colonies and promotes co-mitogenic activity in fetal thymocytes.<sup>15</sup> TSLP functions via a complex of the TSLP receptor and the IL-7 receptor  $\alpha$  chain.<sup>16,17</sup> Those are co-expressed on monocytes, dendritic cells, and T cells.<sup>18</sup> No expression of the TSLP receptor was detected in various nonlymphoid fetal tissues including fetal heart, liver, lung, and kidney.<sup>18</sup>

Here we describe that overexpression of TSLP results in cryoglobulin formation and a systemic inflammatory disease involving the kidney, liver, spleen, lungs, and the skin. We demonstrate that such mice consistently develop a pattern of MPGN closely resembling the disease seen in humans, with a predictable disease course, and which demonstrates a surprising stability of the injury pattern after its induction. This represents the first reproducible mouse model of mixed cryoglobulinemia-associated MPGN.

## Materials and Methods

### Breeding

The establishment of the TSLP transgenic mouse strain (FF8) under the control of the proximal *lck* promoter and details about the development of lymphoid organs in these mice will be described separately (A. Farr, manuscript in preparation). The *lck* gene encodes a lymphocyte-specific protein-tyrosine kinase, p56<sup>lck</sup>. The *lck* proximal promoter is preferentially active in early thymocyte development.<sup>19,20</sup> TSLP transgenic mice were derived from a single founder. Mice were maintained in a specific pathogen-free facility, with food and water *ad libitum*, and under a 12-hour light/dark cycle. All animal studies were reviewed and approved by the Animal Care Committee of the University of Washington, Seattle, WA. TSLP transgenic mice were backcrossed for more than eight generations to a C57BL6 background. TSLP transgenic males were mated with wild-type C57BL6 females. At 3

weeks of age, pups were weaned, labeled by ear-tag, and tail tips were acquired for genotyping.

### Study Design

The main study group consisted of a total of 123 mice, including 61 TSLP transgenic mice and 62 wild-type controls. At least five TSLP transgenic males and five controls were sacrificed at monthly intervals up to 7 months of age (total  $n = 75$ ). An equal number of female mice were sacrificed at 1, 1.5, 2, and 2.5 months of age (total  $n = 48$ ). Furthermore, laboratory data were acquired on an additional series of 27 TSLP transgenic and 16 wild-type controls that were the pilot cohort from which patterns of disease studied in the prospective, serial sacrifice study were first identified.

### Preparation of DNA and Genotyping

The DNeasy tissue kit (Qiagen Inc., Valencia, CA) was used according to the protocol of the manufacturer for DNA isolation. The tail-tips were incubated overnight at 55°C in a mixture containing 180  $\mu$ l of buffer ATL and 20  $\mu$ l of Proteinase K (Qiagen Inc.). After spinning, the supernatant was removed, mixed with 400  $\mu$ l of buffer AL-ethanol buffer mixture (Qiagen Inc.). The mixture was transferred to a DNeasy mini column, centrifuged, and subsequently washed with buffer AW1 and AW2 (Qiagen Inc.). The DNA was eluted in AE buffer (Qiagen Inc.), and the DNA concentration was calculated by the UV absorption at 260 nm. Mice were genotyped using polymerase chain reaction primers: 5'TGCAAGTACTAGTACGGATGGGGC3' from the 5' end of the coding region of the TSLP gene and 5'GGACTTCTTGTGCCA TTTCTGAG3' from the 3' end of the coding region of the TSLP gene. TSLP transgenic animals demonstrate a product of 323 bp. The polymerase chain reaction contained DNA, 1 $\times$  Enzyme Storage Buffer B, 2.5 mmol/L MgCl<sub>2</sub>, 400 nmol/L of each primer, 0.2 mmol/L dNTP, and 1.25 U of *Taq* DNA polymerase (all from Promega Corp., Madison, WI) in a 50- $\mu$ l polymerase chain reaction. Cycling conditions were: 94°C for 2 minutes, followed by 34 cycles of 94°C for 30 seconds, 58°C for 30 seconds, 72°C for 30 seconds and finally 72°C for 5 minutes.

### Tissue Collection

Mice were weighed, anesthetized, and blood was drawn by cardiac puncture into a prewarmed syringe at the time of sacrifice. Spleen, kidneys, liver, lungs, heart, thymus, ears, and bone were collected and portions of each fixed in 10% neutral-buffered formalin, in methyl Carnoys solution (60% methanol, 30% chloroform, 10% acetic acid), in half-strength Karnovsky's solution (1% paraformaldehyde and 1.25% glutaraldehyde in 0.1 mol/L Na cacodylate buffer, pH 7.0) and in part snap-frozen in Tissue-Tek (Sakura Finetek, Torrance, CA). Formalin-fixed and methyl Carnoys-fixed tissues were subsequently embedded in paraffin using routine protocols. Kidneys were sectioned at 2  $\mu$ m and stained using hematoxylin and

**Table 1.** Clinical Data of the Study Group

	Male wild type	Male TSLP transgenic	Female wild type	Female TSLP transgenic
<i>n</i>	38	37	24	24
Body weight (range, g)	10.6–32.0	6.0–31.0	11.0–25.0	6.2–22
Ear involvement	0	22%	0	4%
Cryoglobulins	0	81%	0	90%
Blood urea nitrogen (mg/dl, <i>n</i> = 98)	21.3	25.7*	23.0	29.3*
	( <i>n</i> = 31)	( <i>n</i> = 29)	( <i>n</i> = 21)	( <i>n</i> = 17)
μg Albumin/mg creatinine (±SEM; <i>n</i> = 46)	64 (±11)	150 (±23)*	45 (±14)	245 (±89)*
	( <i>n</i> = 16)	( <i>n</i> = 18)	( <i>n</i> = 7)	( <i>n</i> = 5)
Heart weight (g, % body weight)	0.13 (0.6%)	0.14 (0.6%)	0.1 (0.6%)	0.11 (0.7%)
Kidney weight (g, % body weight)	0.39 (1.7%)	0.31 (1.4%)	0.23 (1.4%)	0.22 (1.4%)
Lung weight (g, % body weight)	0.16 (0.7%)	0.43 <sup>†</sup> (1.9% <sup>†</sup> )	0.16 (0.9%)	0.37 <sup>‡</sup> (2.3% <sup>†</sup> )
Liver weight (g, % body weight)	1.15 (4.9%)	1.43* (6.3% <sup>†</sup> )	0.8 (4.5%)	1.04 (6.6% <sup>†</sup> )
Spleen weight (g, % body weight)	0.08 (1.8%)	0.39 <sup>‡</sup> (3.5% <sup>†</sup> )	0.08 (2.6%)	0.39 <sup>‡</sup> (4.7% <sup>†</sup> )

\**P* < 0.05, <sup>†</sup>*P* < 0.01, <sup>‡</sup>*P* < 0.001, versus wild type.

eosin (H&E), PAS, and periodic acid methenamine silver stain (silver stain).<sup>21</sup> Other organs were embedded in paraffin, cut at 4 μm, and stained with H&E. Snap-frozen kidneys were cut at 6 μm, air-dried, and fixed in ice-cold acetone for 10 minutes.

**Immunofluorescence**

Acetone-fixed sections were air-dried and repeatedly washed in phosphate-buffered saline (PBS; pH 7.4). Sections were incubated with fluorescein-conjugated antibodies against mouse IgA, mouse IgG, mouse IgM, and mouse complement C3 (all from Cappel Pharmaceuticals, Aurora, OH). After subsequent washing steps in

PBS, slides were mounted in Vectashield mounting media (Vector, Burlingame, CA), coverslipped, and viewed in a Zeiss fluorescence microscope. In a blinded manner a semiquantitative score was applied to describe the fluorescence intensity (0, negative; 1, weak; 2, moderate; 3, strong).

**Immunohistochemistry**

The protocols for immunohistochemistry have previously been described in detail.<sup>22,23</sup> T cells were detected using a monoclonal rat anti-CD3 antibody (clone number CD3-2; Serotec, Raleigh, NC), glomerular macrophages were detected using a rat anti-mouse MAC-2 antibody

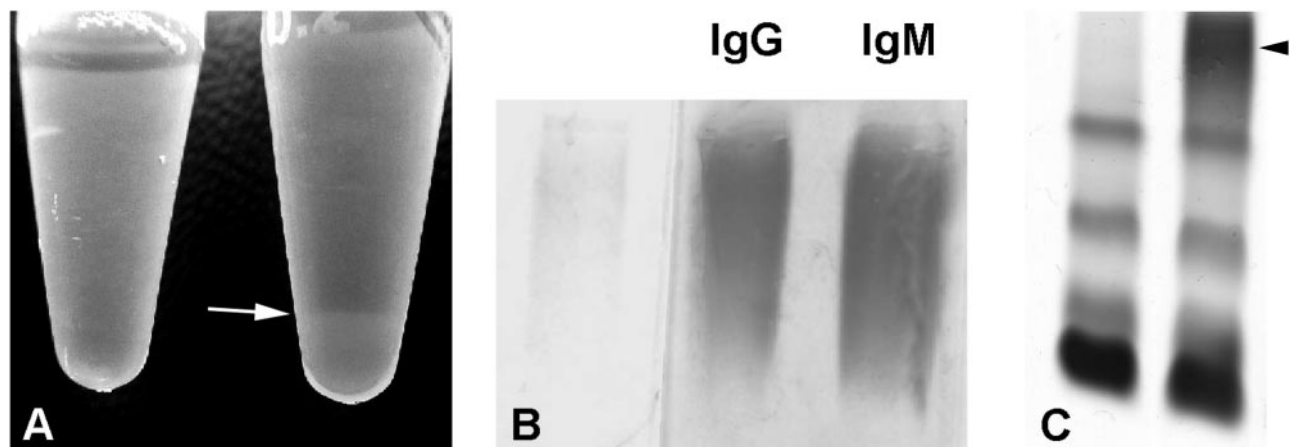
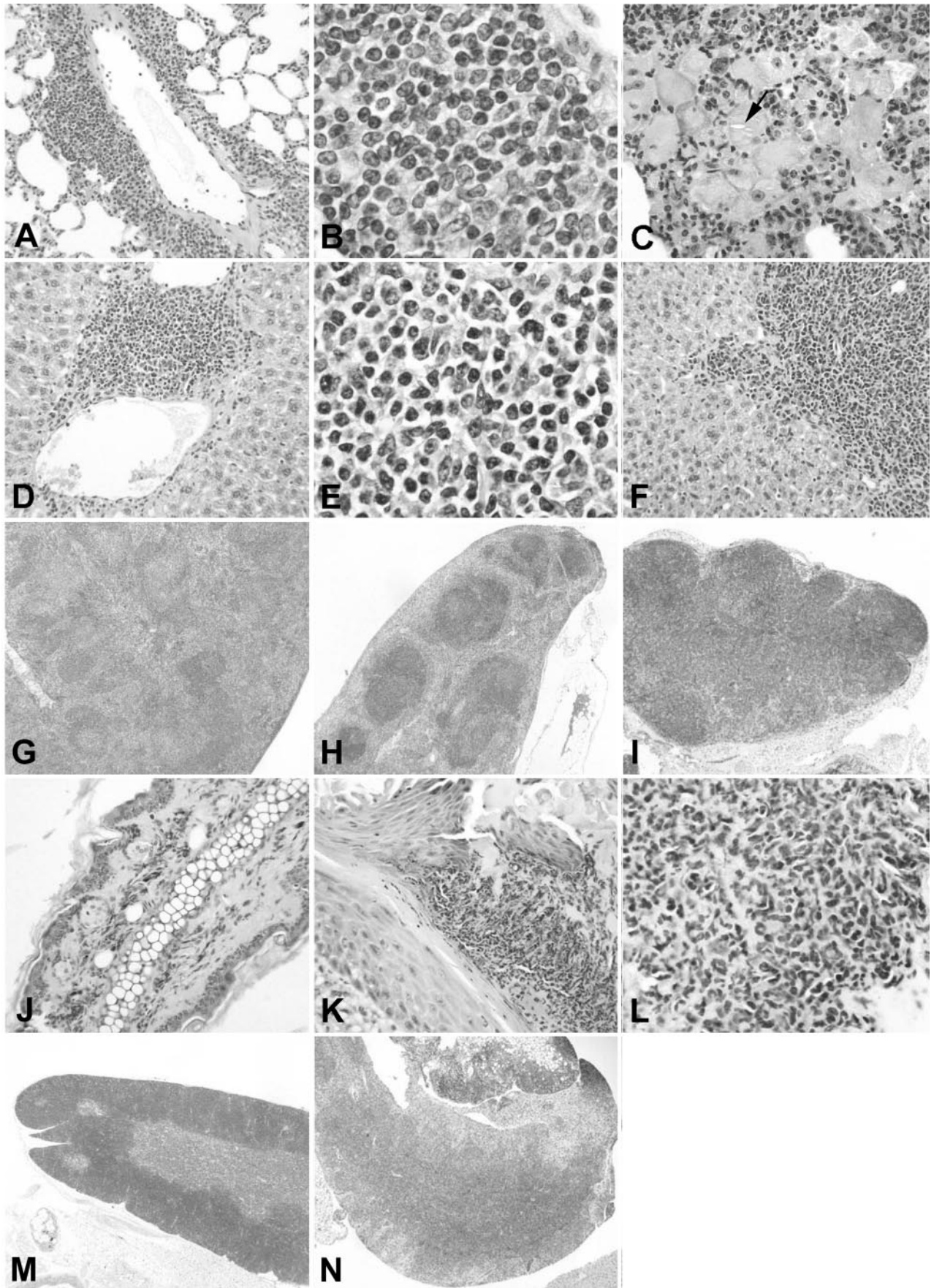


**Figure 1.** A: Sera from a wild-type mouse (left) and a TSLP transgenic mouse (right) after storage at 4°C. The serum on the right demonstrates a cryoprecipitate (arrow). B: Electrophoresis and immunofixation of the cryoprecipitate of a TSLP transgenic mouse illustrates polyclonal IgG and polyclonal IgM, consistent with mixed cryoglobulins (type III). C: Serum protein electrophoresis of a TSLP transgenic male (right) and a wild-type littermate (left). The serum from the TSLP transgenic mouse shows a prominent polyclonal γ-globulin increase (arrowhead). D: Spleen from a wild-type (left) and a TSLP transgenic mouse (right) illustrates the prominent enlargement of the spleen. E: Kidneys from a TSLP transgenic mouse of normal size. Note the impression of the superior surface of the left kidney that resulted from the massive enlargement of the spleen (right).



(Cederlane, Ontario, Canada<sup>24</sup>), B cells were detected using a monoclonal rat anti-mouse CD45 RA antibody (Pharmingen, San Diego, CA), and leukocytes with an antibody against CD45 common on all leukocytes (clone number 30-F11, Pharmingen).<sup>25</sup> Serial 2- $\mu$ m sections of formalin-fixed or methyl Carnoys-fixed and paraffin-embedded tissue were used. Antigen retrieval by steam heating was performed on deparaffinized and rehydrated slides in Antigen Unmasking Solution (Vector) when necessary. Endogenous peroxidases were blocked by incubation with hydrogen peroxide and endogenous biotin was blocked using an Avidin/Biotin blocking kit (Vector). Incubation with primary antibodies was done for 1 hour or overnight, diluted in PBS containing 1% bovine serum albumin (Sigma, St. Louis, MO). After subsequent washing in PBS the tissue was incubated with the biotinylated secondary antibody (rabbit anti-rat, Vector). The ABC-Elite reagent (Vector) was used for signal amplification and 3,3'-diaminobenzidine with nickel enhancement, resulting in a black color product, was used as chromogen. Slides were counterstained with methyl green, dehydrated, and coverslipped.

### Electron Microscopy

The protocol for tissue preparation and staining for transmission electron microscopy has been described previously.<sup>26</sup> Grids were scanned using a Philips 410 electron microscope (Philips Export BV, Eindhoven, The Netherlands). At least six tubular structures present in the immune deposits in four cases of MPGN were measured in high-magnification electron micrographs ( $\times 7100$  or  $\times 10,400$ ) using a Digimatic caliper (Mitutoyo Corp., Japan) for the calculation of the mean diameter.

### Serum Evaluation (Cryoglobulin Isolation, Immunofixation, Anti-Nuclear Antibodies (ANAs), and Blood Urea Nitrogen)

Blood was allowed to clot at 37°C, and serum was collected after centrifugation at 2800 rpm for 30 minutes. Serum samples were kept at 4°C for several days, and formation of cryoprecipitates were identified by visual inspection. Cryoprecipitates were washed four times with ice-cold 0.85% sodium chloride solution (Fisher Scientific, Pittsburgh, PA) and resuspended in 40  $\mu$ l of a sodium chloride solution. Cryoprecipitates were redissolved at 37°C before further characterization. The components of the cryoprecipitates were evaluated by agarose gel electrophoresis and immunofixation, and the involved Ig isotypes were evaluated using a Mouse

Monoclonal Antibody Isotyping Kit (Life Technologies, Inc., Gaithersburg, MD).

Two  $\mu$ l of serum or cryoprecipitate were applied to 0.8% agarose gels (CLP, San Diego, CA) on gel support film (Bio-Rad Laboratories, Hercules, CA). Proteins were separated by electrophoresis in barbital buffer (50 mmol/L sodium barbital (Sigma), 2 mmol/L calcium lactate, pH 8.6) for 35 minutes. Gels were fixed for 10 minutes in a solution consisting of 83.3% saturated picric Acid (Sigma) and 16.7% glacial acetic acid (Sigma), dried, and stained with amido black (ICN Pharmaceuticals, Inc., Costa Mesa, CA).

Gels for immunofixation were incubated with antibodies against mouse IgG (Vector), mouse IgM (Sigma), mouse kappa light chain (clone EM 34.1, Sigma), and mouse lambda light chain (clone 9A8, Sigma) for 1.5 hours. Gels were subsequently dried, washed in 0.85% sodium chloride solution (Fisher Scientific) for 2 hours, dried, and stained with brilliant blue (Sigma). The Mouse Monoclonal Antibody Isotyping Kit (Life Technologies) was used according to the instructions provided by the manufacturer.

Blood urea nitrogen, a measure of renal excretory function, was measured using a standard clinical chemistry analyzer (LX-20; Beckman Laboratories, Brea, CA). The presence of ANAs were examined using the HEP-2 human epithelial cell line as substrate, and anti-double-stranded DNA (dsDNA) antibodies were detected by binding to the *Crithidia lucilliae* substrate (both from Sanofi Diagnostics Pasteur/BioRad, Redmond, WA). For ANA testing, mouse sera were diluted 1:40, and for dsDNA testing sera were diluted to 1:10. Fluorescein-labeled goat antibodies to mouse IgG (Sigma) were used to detect the murine antibodies bound to the substrate.

### Urinary Albumin and Creatinine

Urine samples were evaluated for proteinuria using the albumin/creatinine ratio. Albuminuria was measured using the Albuwell (Exocell, Inc., Philadelphia, PA) mouse albumin enzyme-linked immunosorbent assay and creatinine using the Creatinine Companion (Exocell) according to the protocols of the manufacturer.

### Analysis and Statistics

Morphometric analysis was performed on H&E- and silver-stained histological sections as well as on histological sections stained for macrophages. In a blinded manner 15 consecutive glomerular cross-sections were photographed using a digital camera (Olympus DP11; Olym-

**Figure 2.** Systemic involvement in TSLP transgenic mice. **A, B,** and **C:** Lungs from TSLP transgenic mice. A perivascular leukocytic infiltrate (**A**) is present in the lung of a TSLP transgenic male without significant involvement of the alveoli. **B:** The higher magnification of **A** illustrates a mixed leukocyte population. **C:** Lung of a TSLP transgenic female at the age of 84 days. The alveoli are filled with large macrophages, some of which contain crystalline material (**arrow**). **D, E,** and **F:** Livers of TSLP transgenic mice. A mixed perivenous leukocyte infiltrate is present in **D** and **E**. Further spreading of the leukocyte infiltrate into the liver parenchyma is illustrated in **F**. **G** and **H:** Spleen of a TSLP transgenic male at the age of 111 days (**G**) and a wild-type control (**H**) at the same magnification. **I:** Enlarged mediastinal lymph node from a TSLP transgenic male at the age of 119 days. **J:** Ear of a wild-type control. **K** and **L:** Ear of a TSLP transgenic male at the age of 142 days demonstrates a prominent leukocyte infiltrate of the cutis. **M:** Thymus of a wild-type control. **N:** Illustrates the mediastinal tissue removed from a TSLP transgenic male at the age of 119 days. Original magnifications:  $\times 40$  (**H, I, M,** and **N**);  $\times 200$  (**A, D, F, J,** and **K**);  $\times 400$  (**C** and **L**);  $\times 1000$  (**B** and **E**).

pus America Inc., Melville, NY), and imported into Image-Pro Plus (Media Cybernetics, Silver Spring, MD). The number of nuclei, the area of mesangial matrix, the area occupied by macrophages (determined by measuring all intracellular areas marked by the macrophage cytoplasmic marker Mac-2), and the glomerular tuft area (independent of the urinary space) were quantified for each glomerular cross-section. Using the InStat program (Version 3.0 for Windows; Intuitive Software for Science, San Diego, CA), the mean numbers were compared using the nonparametric Kruskal-Wallis test and the Dunn's multiple comparison. A  $P < 0.05$  was considered to be statistically significant.

## Results

### *TSLP Transgenic Mice Develop a Characteristic Phenotype*

Wild-type females (C57BL6) were mated with TSLP transgenic males on the same genetic background (backcrossed for more than eight generations). Of 256 mice, born during 8 months, 132 were TSLP transgenic (51.6%) and 124 (48.4%) were wild types. The male to female ratio was 0.98 to 1.02. During this time period 17 mice died spontaneously, 5 transgenic males between 40 and 209 days of age and 12 females between 35 and 99 days of age. The higher and earlier mortality of females led us to separate the study groups by gender and include earlier time points for females.

The most impressive clinical symptoms for the entire cohort were progressive ulcerative lesions of the ears. The first manifestation was usually on the side of the ear-tag. Ear involvement was present in eight males at the time of sacrifice, with an age range from 81 to 203 days, but only in one female, sacrificed at the age of 56 days. Although a prominent symptom, the mice did not seem to be clinically impaired by these lesions. The mean body weights rose with age in all groups, but were slightly lower in transgenic animals as compared to wild-type controls. The difference was more prominent in females and at early time points (eg, at the age of 1 month the mean body weights of females were  $11.7 \pm 0.3$  g for wild-type and  $8.8 \pm 0.8$  g for TSLP transgenic mice, respectively). The TSLP transgenic groups included mice with very low body weights (see range in Table 1).

The most prominent finding during necropsy was a massive enlargement of the spleen, which was found in all TSLP transgenic mice (Table 1 and Figures 1 and 2). The enlarged spleen commonly compressed the upper part of the left kidney (Figure 1E). The mean weight of spleens from TSLP transgenic mice was almost five times that of wild-type controls. Although there was marked splenic hypertrophy, histological examination revealed preservation of splenic architecture and cellular diversity and no evidence of a neoplastic population. Furthermore, TSLP transgenic mice showed significantly higher weights of the lungs and the liver.

The lungs contained a mixed perivascular leukocyte infiltrate early during the disease course (Figure 2, A and

B). Eosinophils formed a significant part of the infiltrating leukocytes. Later the alveoli and interstitial spaces from TSLP transgenic mice were filled with macrophages containing eosinophilic material, and commonly, crystals (Figure 2C). We attribute the principal cause of death during the disease course to the severe lung involvement as most of the alveoli were occluded by this inflammatory infiltrate at late time points. The liver involvement began with small perivenous leukocyte infiltrates, which then increased in size, and infiltrated deeper into the liver parenchyma (Figure 2, D, E, and F). The lesion did not progress to a cirrhotic degeneration of the liver within the time frame of our study. No weight differences were found for the heart, although some TSLP transgenic mice demonstrated a prominent enlargement of the heart, detectable by visual examination at necropsy. The mediastinal tissue was increased because of prominent enlargement of lymph nodes and infiltration by leukocytes (Figure 2, I and N). The normal structure of the thymus was no longer apparent (Figure 2, M and N).

### *TSLP Transgenic Mice Develop Mixed Cryoglobulins and Proteinuria, but only a Minor Decrease in Excretory Renal Function*

One hundred fifteen sera were evaluated for cryoprecipitates. Forty-seven samples contained visible cryoprecipitates after storage at 4°C (Figure 1A). All samples were from TSLP transgenic mice, including 29 of 36 TSLP transgenic males and 18 of 20 TSLP transgenic females undergoing such evaluation. None of the wild-type samples contained visible cryoprecipitates. The cryoprecipitates of selected cases were further evaluated by immunofixation for IgM, IgG, kappa light chains, and lambda light chains ( $n = 9$ , Figure 1). All nine studied cases contained type III cryoglobulins, consisting of polyclonal IgM and polyclonal IgG. Dipstick isotype analysis was performed in six cases. All cryoglobulins were positive for IgG1, IgM, and kappa and lambda light chains. IgG3 was detectable in two cases, IgG2A and IgA were detectable in one case each.

Electrophoresis of serum demonstrated a prominent polyclonal increase of the  $\gamma$  region in TSLP transgenic animals, consistent with a polyclonal B cell activation (Figure 1C).

ANA and dsDNA antibodies were studied in a preliminary cohort of TSLP transgenic mice and controls (see Material and Methods). ANAs were detected in 11 of 25 TSLP transgenic mice, but not in wild-type controls. No dsDNA antibodies were detected in the tested animals. The serological tests and immunofixation of the cryoprecipitates were selectively performed because of the limited amounts of mouse serum obtainable and that were insufficient for a multitude of tests in the same small animal.

Renal function was evaluated by measurement of blood urea nitrogen (Table 1). TSLP transgenic mice of both genders showed a significant increase in blood urea nitrogen compared to wild-type mice (Table 1). Although statistically significant, the differences were

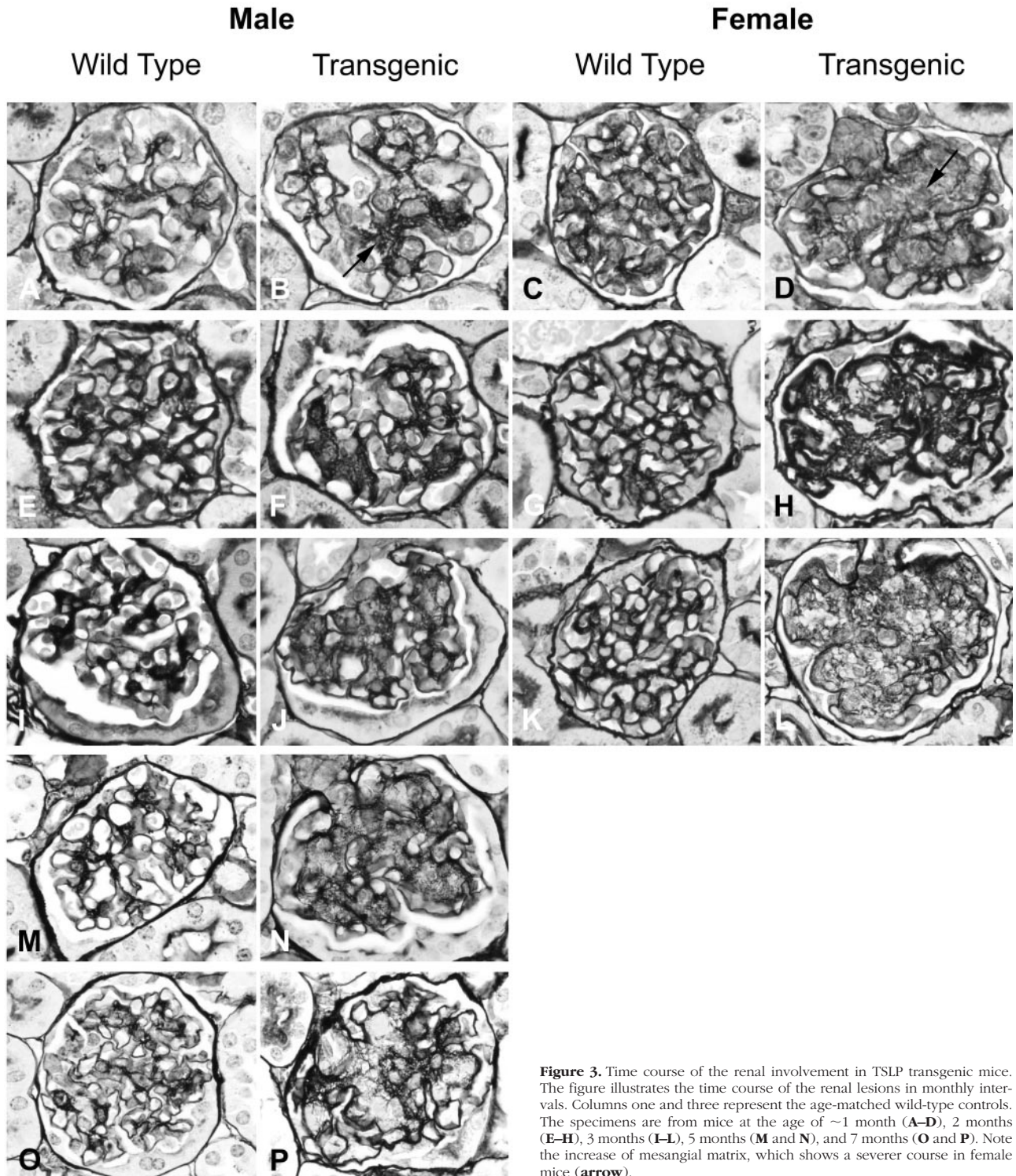


**Figure 3.** Time course of the renal involvement in TSLP transgenic mice. The figure illustrates the time course of the renal lesions in monthly intervals. Columns one and three represent the age-matched wild-type controls. The specimens are from mice at the age of ~1 month (A–D), 2 months (E–H), 3 months (I–L), 5 months (M and N), and 7 months (O and P). Note the increase of mesangial matrix, which shows a severer course in female mice (arrow).

small and the decrease of excretory renal function might therefore not be of clinical importance. Forty-six animals were evaluated for proteinuria at the time of sacrifice. Both genders showed a significantly increased albumin excretion, with an albumin/creatinine ratio increase by ~2.5-fold in TSLP transgenic males and fivefold in TSLP transgenic females compared to wild-type mice (Table 1).

### *TSLP Transgenic Mice Develop a Cryoglobulinemic Glomerulonephritis*

The kidneys appeared macroscopically normal in size, with a normal surface, and the weight was not different compared to wild-type controls.

The time course of the glomerular lesions is illustrated in Figure 3 and the details in Figure 4. After the age of 1

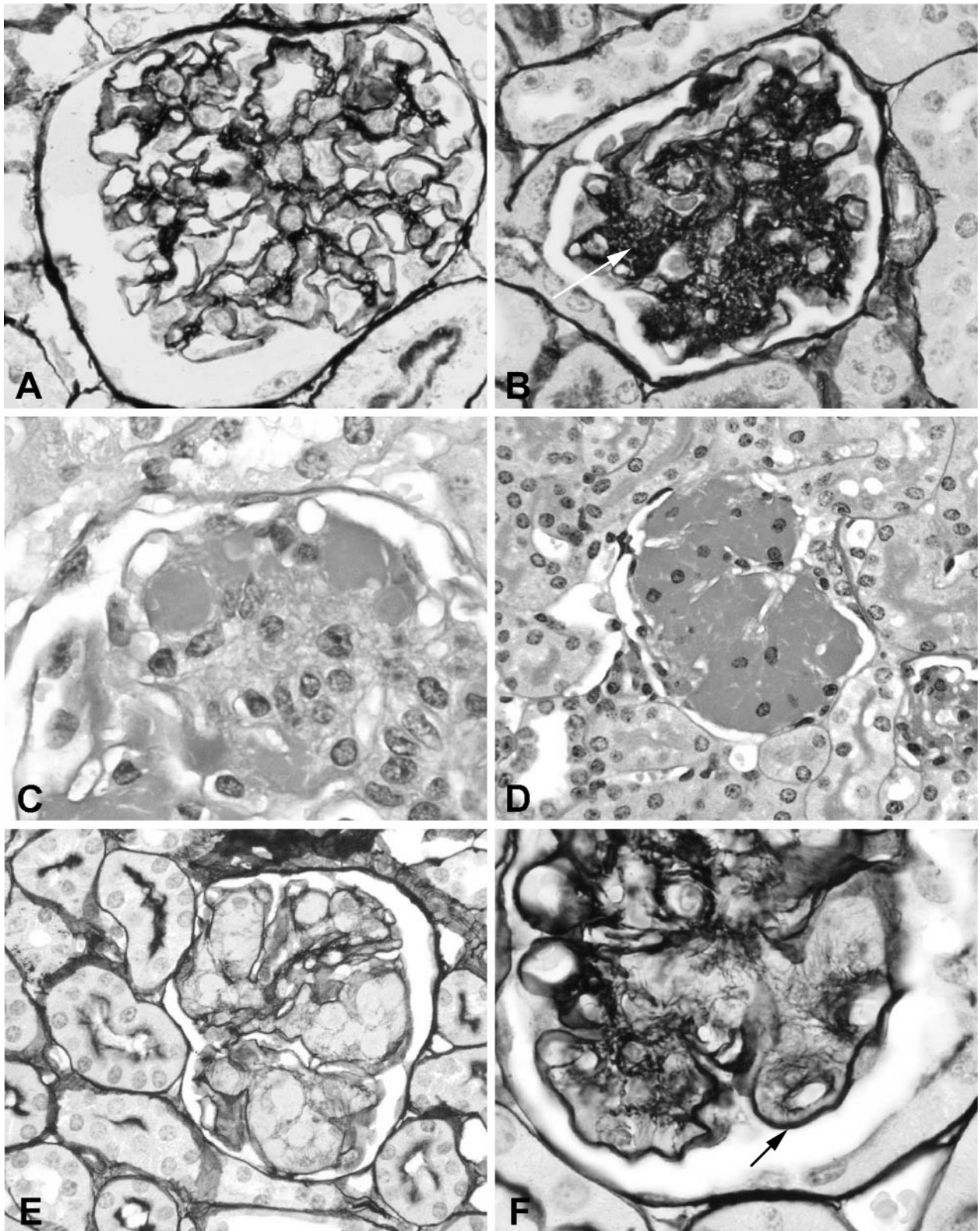


**Figure 4.** Morphological features of renal involvement in TSLP transgenic mice. **A:** Wild-type male at the age of 199 days (silver stain; original magnification,  $\times 1000$ ). **B:** TSLP transgenic female at the age of 71 days. The glomerular tuft shows prominent increase of agyrophilic mesangial matrix (**arrow**; silver stain; original magnification,  $\times 1000$ ). **C and D:** Transgenic male at the age of 140 days. Deposition of PAS-positive material in peripheral capillaries and the mesangium (PAS stain; original magnification,  $\times 1000$ ). **D and E** illustrate the severity of the glomerular lesion with massive deposition of PAS-positive material (**D**) that is not agyrophilic in the silver stain (**E**, original magnification,  $\times 400$ ). Note the normal tubulointerstitium in contrast to the severe glomerular lesion. **F:** Thickened glomerular capillary loop with a double contour (**arrow**) in a 137-day-old TSLP transgenic male (silver stain; original magnification,  $\times 1000$ ).

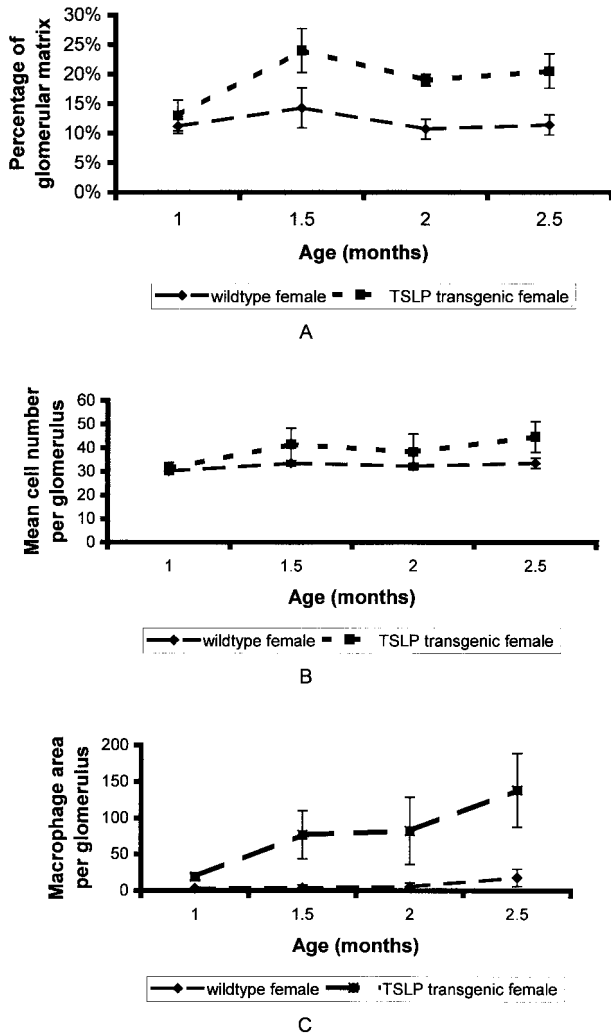


**Figure 5.** Time course of renal lesions in females. **A:** Time course of the percentage of glomerular matrix per glomerulus. **B:** Time course of the mean number of glomerular cells. **C:** Time course of macrophage infiltration expressed as mean area of macrophages per glomerulus ( $\mu\text{m}^2$  per glomerulus).

month all TSLP transgenic animals demonstrated renal lesions. TSLP transgenic mice of both genders showed a widening of the mesangial area. This was because of an increase in mesangial matrix and mesangial deposits of immune complexes. The deposits could be distinguished on silver staining by lack of reactivity with the silver stain, unlike the silver staining of mesangial matrix (Figure 4, B and E). No prominent increase in glomerular cell numbers was apparent. The widening of the mesangial area became apparent during the first month of age, and was more prominent in females at early time points (eg, 1 to 2 months of age) than in males (Figures 3 and 4B). Capillary walls were thickened, sometimes with prominent double contours of the capillary walls, as revealed by silver stains (Figures 3H and 4F). PAS-positive deposits were present in the mesangium and in capillary walls. These deposits narrowed the capillary lumina, and these intracapillary globular thrombi appeared to cause complete capillary occlusion (Figure 4, C and D). Therefore, with progression of the disease course the number of patent capillary lumina decreased. A lobular accentua-

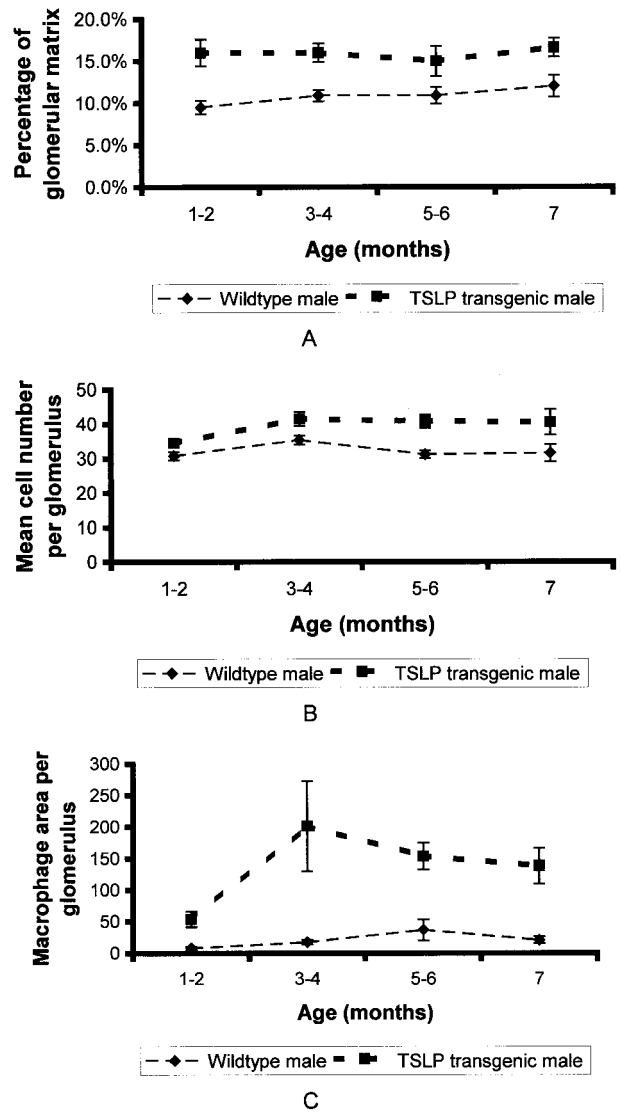


**Figure 6.** Time course of renal lesions in males. **A:** Time course of the percentage of glomerular matrix per glomerulus. **B:** Time course of the mean number of glomerular cells. **C:** Time course of macrophage infiltration expressed as mean area of macrophages per glomerulus ( $\mu\text{m}^2$  per glomerulus).

tion of the glomerular tuft architecture was commonly apparent. In the most severe cases, the mesangium was widened, and most of the capillary lumina were occluded. In contrast, globally sclerotic glomeruli were absent and the tubulointerstitium was well preserved in all cases, without significant inflammation or fibrosis (Figure 4, D and E). No leukocytic infiltrates were found in arterial walls.

The morphological findings for the glomerular tuft area, glomerular matrix area, and glomerular cellularity were quantified by morphometry (Figures 5 and 6, and Table 2). TSLP transgenic mice demonstrated a significant increase in the proportion of each glomerulus occupied by extracellular matrix (Table 2). The glomerular tuft area was increased in TSLP transgenic animals of both genders, but the difference compared to wild-type controls reached the level of significance only in male mice. The cell number per glomerulus was significantly increased in

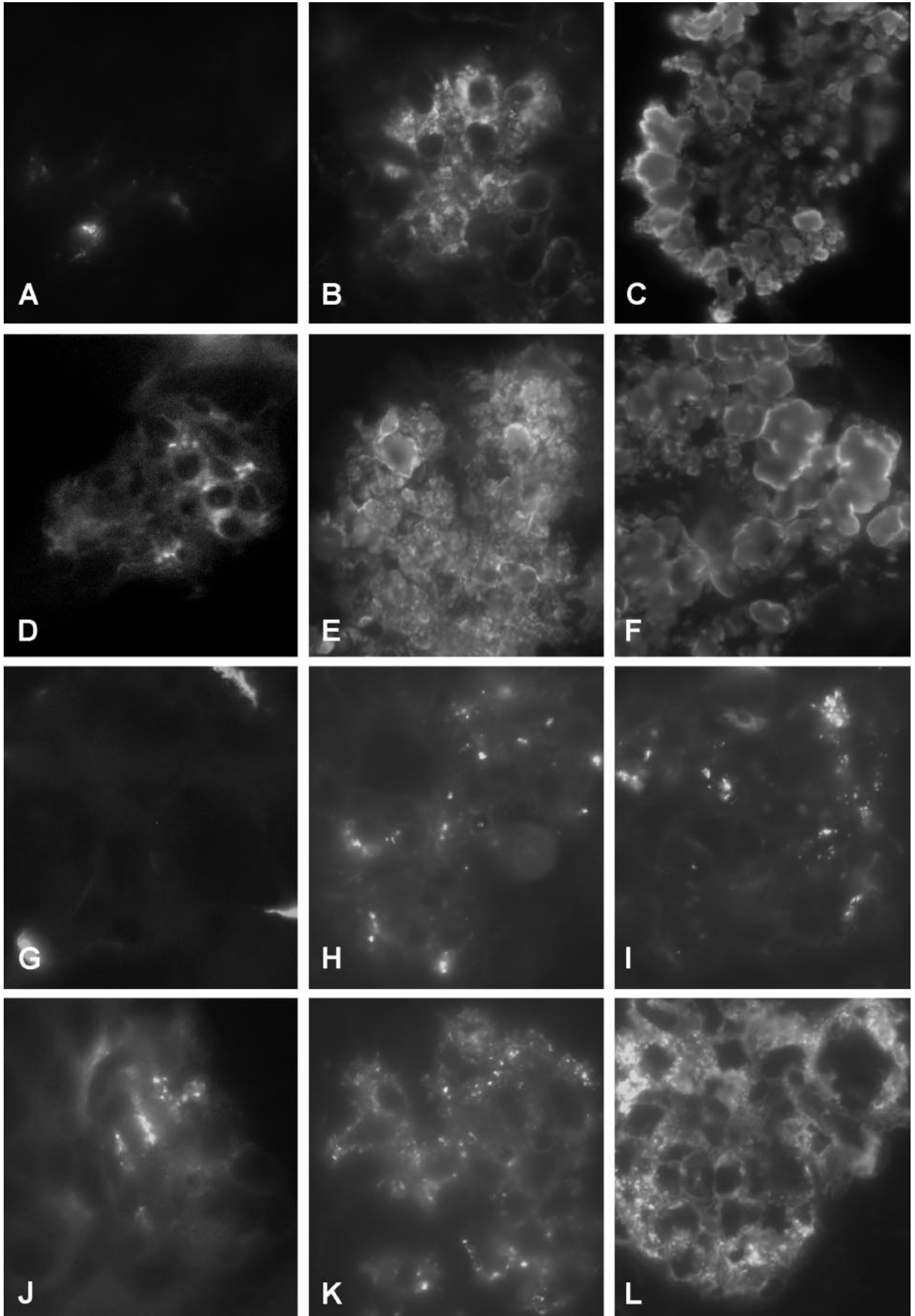


**Table 2.** Morphometric Data of the Renal Morphology

	Male wild type	Male TSLP transgenic	Female wild type	Female TSLP transgenic
Mean matrix area per glomerulus ( $\mu\text{m}^2 \pm \text{SEM}$ )	227.2 ( $\pm 14.4$ )	469.8 <sup>†</sup> ( $\pm 40.4$ )	201.9 ( $\pm 26.7$ )	413 <sup>†</sup> ( $\pm 41.2$ )
Mean glomerular tuft area ( $\mu\text{m}^2 \pm \text{SEM}$ )	1623 ( $\pm 145$ )	2223* ( $\pm 218.5$ )	1188 ( $\pm 177.1$ )	1450 ( $\pm 199.1$ )
Percentage of glomerular matrix	11% ( $\pm 0.46$ )	16% <sup>†</sup> ( $\pm 0.74$ )	12% ( $\pm 0.93$ )	19% <sup>†</sup> ( $\pm 1.5$ )
Mean cells per glomerulus ( $\pm \text{SEM}$ )	32.3 ( $\pm 0.73$ )	39.1 <sup>†</sup> ( $\pm 1.07$ )	32.4 ( $\pm 0.72$ )	39* ( $\pm 1.56$ )
Mean cells per glomerular tuft area (cells/ $\mu\text{m}^2 \pm \text{SEM}$ )	0.016 ( $\pm 0.0005$ )	0.015 ( $\pm 0.0006$ )	0.019 ( $\pm 0.0007$ )	0.017 ( $\pm 0.0007$ )
Area of macrophages per glomerulus ( $\pm \text{SEM}$ )	20.2 ( $\pm 4.8$ )	136.1 <sup>†</sup> ( $\pm 24.2$ )	7.7 ( $\pm 3.4$ )	79.2 <sup>†</sup> ( $\pm 19.8$ )
Percentage of glomerular macrophage area ( $\pm \text{SEM}$ )	0.7% ( $\pm 0.16$ )	3.7% <sup>†</sup> ( $\pm 0.4$ )	0.3% ( $\pm 0.1$ )	2.7% <sup>†</sup> ( $\pm 0.5$ )

\* $P < 0.05$ , <sup>†</sup> $P < 0.01$  versus wild type.

TSLP transgenic animals, but the cell number adjusted for glomerular tuft area did not change during the disease course. Therefore, the lesion in TSLP transgenic mice is characterized by increased glomerular size, an absolute increase in the cell number per glomerulus, and an increase of glomerular extracellular matrix. The time course covering the first 2 months in females and the first 7 months in males (Figures 5 and 6) illustrates that the increase in extracellular matrix and in cells per glomerulus took place at the onset of the disease course, within the first 2 months, and then reached a plateau. Both features seemed to be more pronounced in TSLP transgenic females as compared to males at early time points.

Glomerular immune deposits were characterized by immunofluorescence microscopy on frozen tissue sections for mouse IgG, IgM, IgA, and complement C3 deposits (Figure 7 and Table 3). Mild to moderate deposition of all three Igs were detectable in wild-type controls and were pronounced in males as compared to females. C3 deposition was only occasionally detected in glomeruli from wild-type mice. Compared with wild-type mice, TSLP transgenic mice demonstrated Ig deposits with greater fluorescence signals. TSLP transgenic females demonstrated significantly increased scores for all three types of Igs and C3, in TSLP transgenic males the scores for IgG, IgA, and C3 were significantly elevated (Table 3, Figure 7). The deposits were found in the mesangium and in peripheral glomerular capillaries with a granular pattern of deposition. Some cases contained IgM in deposits that filled capillary lumina (comparable in shape to the described PAS-positive globular deposits). In these cases the glomerular distribution of IgG (Figure 7, E and F) and C3 (Figure 7, H and I) was similar to the IgM distribution pattern. However, C3 staining was weaker and more focal in nature compared with IgG and IgM staining. In addition to glomerular deposits, TSLP transgenic animals demonstrated immunoreactivity of all three Ig classes in the peritubular interstitium. In contrast, interstitial C3 deposition was weak or absent, without differences between wild-type and TSLP transgenic animals.

Infiltrating leukocytes were characterized by immunohistochemistry using a pan-leukocyte marker, as well as markers for B cells, T cells, and macrophages. Macrophages were the main cell population infiltrating glomeruli. Glomerular T and B cells were only occasionally seen, without prominent differences between TSLP transgenic mice and wild-type controls. The quantification of the number of macrophages is problematic by immunohistochemistry, because of positive color products on cell portions of macrophages incompletely present in a given plane of section. Therefore, we summarized the total area of positive color product in each glomerulus as a measure of the severity of macrophage infiltration. The area occupied by macrophages per glomerulus as well as per glomerular tuft area was significantly increased in TSLP transgenic mice as compared to wild-type controls (Table 2). The area occupied by macrophages rose progressively in TSLP transgenic females during the first 3 months of life (Figure 5). In males the macrophage area peaked during the third and fourth month of life and then gradually decreased (Figure 6).

The ultrastructure of the renal lesions was further evaluated by transmission electron microscopy in selected cases (Figures 8 and 9). Electron-dense immune deposits were apparent in the mesangium as well as in the subendothelial space in TSLP transgenic mice (Figure 8). Podocyte foot processes were usually well preserved, but foot process effacement was seen in areas of capillary walls involved by immune deposits (Figure 8, A and C). The endothelial cells covering the immune deposits demonstrated signs of activation, with cellular swelling and absence of the normal pores. Subendothelial deposits and cellular interposition were accompanied by splitting of capillary walls. Leukocytes were present in capillary lumina, some adherent to endothelial cells, and some were found infiltrating the mesangium. Occasional basophils were seen in the capillary lumen and in the mesangium. At higher magnification the deposits commonly demonstrated organization in the form of microtubules arranged in arrays (Figures 8C and 9). Measurement of

**Figure 7.** Characterization of the immune deposits by immunofluorescence. **A, D, G, and J:** Renal specimens from a wild-type female stained for IgM (**A**), IgG (**D**), C3 (**G**), and IgA (**J**). The tissue shows weak and focal positivity for IgM and IgG, no glomerular C3 deposition, and positivity for IgA. **B, E, H, and K:** Renal specimen from a TSLP transgenic female stained for IgM (**B**), IgG (**E**), C3 (**H**), and IgA (**K**). Strong granular IgM and IgG deposits can be detected in the mesangium and in capillary walls. Focal C3 deposits can be seen in the same distribution. **C, F, I, and L:** Renal specimen from a TSLP transgenic male stained for IgM (**C**), IgG (**F**), C3 (**I**), and IgA (**L**).

**Table 3.** Mean Immunofluorescence Scores for the Glomerular Deposition of IgG, IgM, C3, and IgA

	Male wild type	Male TSLP transgenic	Female wild type	Female TSLP transgenic
Mean IgG scores ( $\pm$ SEM)	1.7 ( $\pm 0.13$ , $n = 34$ )	2.8 <sup>†</sup> ( $\pm 0.08$ , $n = 27$ )	0.9 ( $\pm 0.12$ , $n = 20$ )	2* ( $\pm 0.12$ , $n = 16$ )
Mean IgM scores ( $\pm$ SEM)	1.8 ( $\pm 0.14$ , $n = 34$ )	2.2 ( $\pm 0.12$ , $n = 29$ )	1.4 ( $\pm 0.14$ , $n = 19$ )	2.4* ( $\pm 0.18$ , $n = 13$ )
Mean C3 scores ( $\pm$ SEM)	1.2 ( $\pm 0.16$ , $n = 34$ )	2.5 <sup>†</sup> ( $\pm 0.12$ , $n = 30$ )	0.4 ( $\pm 0.14$ , $n = 19$ )	1.8* ( $\pm 0.24$ , $n = 14$ )
Mean IgA scores ( $\pm$ SEM)	1.8 ( $\pm 0.12$ , $n = 34$ )	2.8 <sup>†</sup> ( $\pm 0.07$ , $n = 31$ )	1.5 ( $\pm 0.11$ , $n = 19$ )	2.8* ( $\pm 0.1$ , $n = 13$ )

\* $P < 0.01$ , <sup>†</sup> $P < 0.001$  versus wild type.

these tubules in four cases revealed an approximate mean diameter of 41, 44, 53, and 55 nm.

### Discussion

MPGN, also referred to by some authors as mesangio-capillary glomerulonephritis, is a histopathological entity characterized by: 1) thickening of peripheral capillary walls with subendothelial immune deposits and/or intramembranous dense deposits of undefined origin; 2) histologically apparent splitting or reduplication of the basement membranes that often occurs as a result of cellular interposition between the split basement membranes; and 3) glomerular mesangial expansion because of both increased cellularity and increased matrix, with an accentuated lobular appearance of the glomerular tuft.<sup>27,28</sup> Two major types of idiopathic MPGN in humans have been identified, usually referred to as type I and type II.<sup>27,28</sup> The pathogenetic basis of type I, by far the most common manifestation of MPGN, is the deposition of mesangial and subendothelial immune complexes that is reflected by finding discrete immune reactants and/or components of the complement cascade in this distribution by immunofluorescence microscopy, as well as the presence of discrete electron-dense deposits in the same distribution visualized by electron microscopy. Type II is an uncommon and somewhat obscure entity also known as dense deposit disease, which is not related to Ig deposition and has no clear relationship to the disease seen in TSLP transgenic mice.

MPGN has been described as a secondary consequence of a wide range of underlying diseases, primarily by those with chronic antigenemia, such as infected ventriculoatrial shunts (shunt nephritis) or endocarditis, chronic viral infections (eg, hepatitis virus), parasitic infections (eg, malaria, schistosomiasis), and systemic immune complex diseases such as systemic lupus erythematosus and cryoglobulinemia.<sup>29</sup>

Mixed cryoglobulinemia, especially in the context of hepatitis C virus infection, is currently thought to be a common, and perhaps the most common underlying disease in which MPGN type I is encountered.<sup>12</sup> An opportunity to study the development and evolution of mixed cryoglobulinemia is particularly relevant to an understanding of the pathogenesis of MPGN type I. Our knowledge about the pathogenesis of MPGN is still severely limited because of a lack of available, relevant animal

models.<sup>30</sup> MPGN has been described in large animals such as Finnish Landrace lambs,<sup>31–33</sup> dogs,<sup>34–37</sup> horses,<sup>38</sup> and pigs.<sup>39–42</sup> Although some of these diseases are inherited and have defined genetic defects such as complement deficiency, these systems have limited utility for most investigators, because of such factors as limited availability of reagents to characterize cells and peptides in these species, the need for special animal care facilities to maintain such large animals with resultant large expenses, and the time required to breed sufficient animals to perform interventional studies with large enough cohorts to be statistically significant. We know of only one mouse model of MPGN that has been described, the sph<sup>ha</sup>/sph<sup>ha</sup> mice with congenital hemolytic anemia, but this model has not been subjected to extensive subsequent studies.<sup>43</sup>

In this study we describe a reproducible MPGN model in a transgenic mouse strain that might help to overcome some of the mentioned limitations of other models. All TSLP transgenic mice developed glomerular lesions as early as the first month of life. By 50 days of age females already show a very prominent histological lesion of MPGN. Consistent with a MPGN pattern, TSLP transgenic mice develop subendothelial immune deposits, splitting with cellular interposition of capillary walls, and an accentuated lobular appearance of the glomerular tuft. Furthermore, the deposition pattern of Igs and C3 is similar to the human disease. These features make this mouse strain a very attractive MPGN model and enable detailed pathogenetic studies by inbreeding of genetically modified murine strains.

TSLP transgenic mice develop MPGN in the context of type III cryoglobulins and demonstrate the most typical features of cryoglobulinemic glomerulonephritis. There are reported examples of murine hybridomas that have produced cryoprecipitable Igs analogous to type I cryoglobulins in humans, but infusion studies of these Igs have not resulted in production of MPGN-like lesions in animals.<sup>44</sup> Another approach has been to use human cryoglobulins removed by therapeutic aphereses, to purify them, and reinfuse the cryoglobulins into rodents. Infusion of some of these cryoglobulins has resulted in glomerular lesions similar to those encountered in the patients from whom they were derived.<sup>45</sup> Although an interesting proof of principle, these models are limited in their availability for extended use in studies of pathogenesis or therapeutic interventions. In addition to the fea-

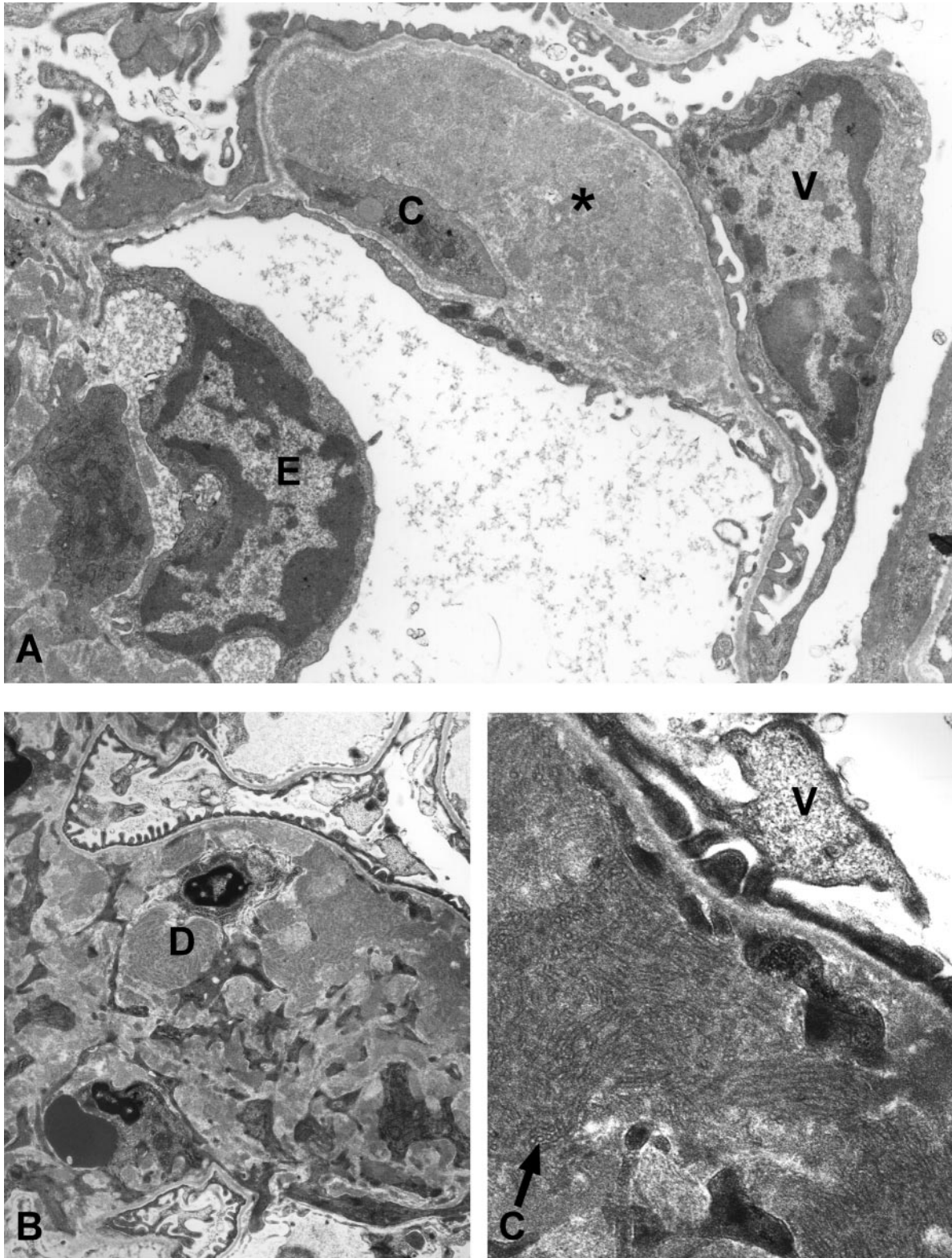


**Figure 8.** Ultrastructural features of TSLP transgenic females. **A:** Transmission electron microscopy of a specimen from a 1-month-old TSLP transgenic female. The glomerular capillary shows a large subendothelial electron-dense deposit (**asterisk**), and cellular interposition (**C**). Note effacement of the foot processes over the deposit (**V**, visceral epithelial cell; **E**, endothelial cell). **B** and **C:** Transmission electron microscopy of a renal specimen from a 2-month-old TSLP transgenic female. Widening of the mesangial area because of increased matrix, and electron-dense deposits (**D**, deposit), with a tubular ultrastructure at higher magnification (**arrow** in **C**) (**V**, visceral epithelial cell). Original magnifications:  $\times 4400$  (**A** and **B**);  $\times 16,900$  (**C**).

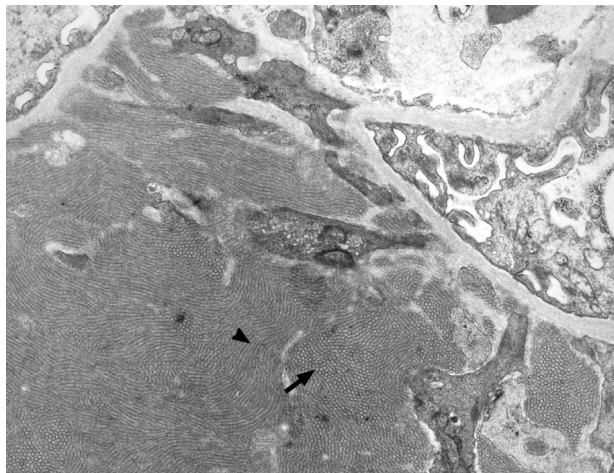


**Figure 9.** Microtubular ultrastructure of immune deposits in a TSLP transgenic male. Transmission electron microscopy of a specimen from a 199-day-old TSLP transgenic male (original magnification,  $\times 7100$ ). Note the prominent microtubular organization of the large mesangial immune deposit. The deposits demonstrate annular appearance on transverse sections (arrow) and a cylindrical on longitudinal sections (arrowhead).

tures of idiopathic MPGN, cryoglobulinemia-associated cases show a prominent macrophage influx and occlusion of glomerular capillaries by PAS-positive material, corresponding to precipitates of the complexed Igs.<sup>12,46</sup> Both features were present in TSLP transgenic mice.

Another characteristic feature of cryoglobulin deposition in the kidney is an ultrastructural organization of the Igs detectable by electron microscopy. Tubular, fibrillar, and fingerprint features, as well as cylindrical and annular organization of the deposits have been described in humans.<sup>47–53</sup> Commonly the electron-dense deposits in TSLP transgenic mice demonstrated a microtubular appearance with annular structures on transverse sections and a cylindrical appearance on longitudinal sections. Therefore the ultrastructure of the electron-dense deposits closely resembles the description of some mixed cryoglobulins occurring in humans.

TSLP transgenic female mice developed a more severe phenotype than TSLP transgenic males, resulting in severer renal lesions early in the disease course and a higher mortality as compared to males. The prevalence of detectable amounts of cryoglobulins was slightly higher in females, and consistent with this finding female gender has been described as a risk factor for hepatitis C-associated cryoglobulinemia.<sup>10</sup> Furthermore, gender differences with a female predominance have been described in various human and experimental autoimmune diseases.<sup>54,55</sup> B-cell hyperactivity with increased synthesis of Igs including autoantibodies has been described in estrogen-treated mice, a mechanism that might be of importance in our model.<sup>56</sup> The exact cause for the gender differences in TSLP transgenic mice, although consistent with other models of autoimmune diseases remain speculative and need to be addressed in further studies.

In summary, we present the first transgenic mouse model of mixed cryoglobulinemia (type III) that closely resembles important aspects of the human disease. The renal lesion is characterized by mesangial expansion

because of matrix and immune complex deposition, capillary wall thickening (by immune deposits and cellular interposition), occlusion of capillary lumina by subendothelial deposits and intraluminal PAS-positive material, and macrophage influx. Therefore, TSLP transgenic mice will enable detailed studies on the pathogenetic events of the membranoproliferative pattern of glomerulonephritis, as well as the evaluation of functional roles of cytokines and growth hormones by crossbreeding with other genetically manipulated mouse strains on the same defined genetic background.

### Acknowledgments

We thank Tracy Goodpaster and Erik A. Hughes for technical assistance.

### References

1. Ramos-Casals M, Trejo O, Garcia-Carrasco M, Cervera R, Font J: Mixed cryoglobulinemia: new concepts. *Lupus* 2000, 9:83–91
2. Cacoub P, Renou C, Rosenthal E, Cohen P, Loury I, Loustaud-Ratti V, Yamamoto AM, Camproux AC, Hausfater P, Musset L, Veyssier P, Raguin G, Piette JC: Extrahepatic manifestations associated with hepatitis C virus infection. A prospective multicenter study of 321 patients. The GERMIVIC. *Groupe d'Etude et de Recherche en Médecine Interne et Maladies Infectieuses sur le Virus de l'Hépatite C. Médecine* 2000, 79:47–56
3. Sinico RA, Fornasieri A, D'Amico G: Renal manifestations associated with hepatitis C virus. *Ann Med Interne* 2000, 151:41–45
4. Kallemmuchikkal U, Gorevic PD: Evaluation of cryoglobulins. *Arch Pathol Lab Med* 1999, 123:119–125
5. Dispenzieri A, Gorevic PD: Cryoglobulinemia. *Hematol Oncol Clin North Am* 1999, 13:1315–1349
6. Lamprecht P, Gause A, Gross WL: Cryoglobulinemic vasculitis. *Arthritis Rheum* 1999, 42:2507–2516
7. Brouet JC, Clauvel JP, Danon F, Klein M, Seligmann M: Biologic and clinical significance of cryoglobulins. A report of 86 cases. *Am J Med* 1974, 57:775–788
8. Della Rossa A, Trevisani G, Bombardieri S: Cryoglobulins and cryoglobulinemia. Diagnostic and therapeutic considerations. *Clin Rev Allergy Immunol* 1998, 16:249–264
9. Gorevic PD, Kassab HJ, Levo Y, Kohn R, Meltzer M, Prose P, Franklin EC: Mixed cryoglobulinemia: clinical aspects and long-term follow-up of 40 patients. *Am J Med* 1980, 69:287–308
10. Cicardi M, Cesana B, Del Ninno E, Pappalardo E, Silini E, Agostoni A, Colombo M: Prevalence and risk factors for the presence of serum cryoglobulins in patients with chronic hepatitis C. *J Viral Hepatol* 2000, 7:138–143
11. Johnson RJ, Willson R, Yamabe H, Couser W, Alpers CE, Wener MH, Davis C, Gretch DR: Renal manifestations of hepatitis C virus infection. *Kidney Int* 1994, 46:1255–1263
12. D'Amico G: Renal involvement in hepatitis C infection: cryoglobulinemic glomerulonephritis. *Kidney Int* 1998, 54:650–671
13. Rastaldi MP, Ferrario F, Crippa A, Dell'Antonio G, Casartelli D, Grillo C, D'Amico G: Glomerular monocyte-macrophage features in ANCA-positive renal vasculitis and cryoglobulinemic nephritis. *J Am Soc Nephrol* 2000, 11:2036–2043
14. Friend SL, Hosier S, Nelson A, Foxworthe D, Williams DE, Farr A: A thymic stromal cell line supports in vitro development of surface IgM+ B cells and produces a novel growth factor affecting B and T lineage cells. *Exp Hematol* 1994, 22:321–328
15. Sims JE, Williams DE, Morrissey PJ, Garka K, Foxworthe D, Price V, Friend SL, Farr A, Bedell MA, Jenkins NA, Copeland NG, Grabstein K, Paxton RJ: Molecular cloning and biological characterization of a novel murine lymphoid growth factor. *J Exp Med* 2000, 192:671–680
16. Pandey A, Ozaki K, Baumann H, Levin SD, Puel A, Farr AG, Ziegler SF, Leonard WJ, Lodish HF: Cloning of a receptor subunit required for

- signaling by thymic stromal lymphopoietin. *Nat Immunol* 2000, 1:59–64
17. Park LS, Martin U, Garka K, Glianiak B, Di Santo JP, Muller W, Lar-gaespada DA, Copeland NG, Jenkins NA, Farr AG, Ziegler SF, Morrissey PJ, Paxton R, Sims JE: Cloning of the murine thymic stromal lymphopoietin (TSLP) receptor: formation of a functional heteromeric complex requires interleukin 7 receptor. *J Exp Med* 2000, 192:659–670
  18. Reche PA, Soumelis V, Gorman DM, Clifford T, Liu M, Travis M, Zurawski SM, Johnston J, Liu YJ, Spits H, de Waal Malefyt R, Kaste-lein RA, Bazan JF: Human thymic stromal lymphopoietin preferentially stimulates myeloid cells. *J Immunol* 2001, 167:336–343
  19. Wildin RS, Garvin AM, Pawar S, Lewis DB, Abraham KM, Forbush KA, Ziegler SF, Allen JM, Perlmutter RM: Developmental regulation of lck gene expression in T lymphocytes. *J Exp Med* 1991, 173:383–393
  20. Shimizu C, Kawamoto H, Yamashita M, Kimura M, Kondou E, Kaneko Y, Okada S, Tokuhisa T, Yokoyama M, Taniguchi M, Katsura Y, Nakayama T: Progression of T cell lineage restriction in the earliest subpopulation of murine adult thymus visualized by the expression of lck proximal promoter activity. *Int Immunol* 2001, 13:105–117
  21. Min W, Yamanaka N: Three-dimensional analysis of increased vas-culature around the glomerular vascular pole in diabetic nephropathy. *Virchows Arch A Pathol Anat Histopathology* 1993, 423:201–207
  22. Segerer S, Cui Y, Hudkins KL, Goodpaster T, Eitner F, Mack M, Schlondorff D, Alpers CE: Expression of the chemokine monocyte chemoattractant protein-1 and its receptor chemokine receptor 2 in human crescentic glomerulonephritis. *J Am Soc Nephrol* 2000, 11: 2231–2242
  23. Segerer S, Cui Y, Eitner F, Goodpaster T, Hudkins KL, Mack M, Cartron JP, Colin Y, Schlondorff D, Alpers CE: Expression of chemo-kines and chemokine receptors during human renal transplant rejection. *Am J Kidney Dis* 2001, 37:518–531
  24. Bird JE, Giancarli MR, Kurihara T, Kowala MC, Valentine MT, Gitlitz PH, Pandya DG, French MH, Durham SK: Increased severity of glomerulonephritis in C-C chemokine receptor 2 knockout mice. *Kidney Int* 2000, 57:129–136
  25. Ledbetter JA, Herzenberg LA: Xenogeneic monoclonal antibodies to mouse lymphoid differentiation antigens. *Immunol Rev* 1979, 47: 63–90
  26. Alpers CE, Hudkins KL, Pritzl P, Johnson RJ: Mechanisms of clear-ance of immune complexes from peritubular capillaries in the rat. *Am J Pathol* 1991, 139:855–867
  27. D'Amico G, Ferrario F: Mesangiocapillary glomerulonephritis. *J Am Soc Nephrol* 1992, 2:S159–S166
  28. Jones DB: Membranoproliferative glomerulonephritis. One of many diseases? *Arch Pathol Lab Med* 1977, 101:457–461
  29. Zamurovic D, Churg J: Idiopathic and secondary mesangiocapillary glomerulonephritis. *Nephron* 1984, 38:145–153
  30. Wilson CB: Immune models of glomerular injury. *Immunologic Renal Diseases*. Edited by EG Neilson, WG Couser. Philadelphia, Lippin-cott-Raven Publishers, 1997, pp 729–773
  31. Angus KW, Gardiner AC, Mitchell B, Thomson D: Mesangiocapillary glomerulonephritis in lambs: the ultrastructure and immunopathology of diffuse glomerulonephritis in newly born Finnish Landrace lambs. *J Pathol* 1980, 131:65–74
  32. Angus KW, Gardiner AC, Morgan KT, Gray EW, Thomson D: Mesan-giocapillary glomerulonephritis in lambs. II. Pathological findings and electron microscopy of the renal lesions. *J Comp Pathol* 1974, 84: 319–330
  33. Angus KW, Sykes AR, Gardiner AC, Morgan KT, Thomson D: Mesan-giocapillary glomerulonephritis in lambs. I. Clinical and biochemical findings in a Finnish Landrace flock. *J Comp Pathol* 1974, 84:309–317
  34. Minkus G, Breuer W, Wanke R, Reusch C, Leuterer G, Brem G, Hermanns W: Familial nephropathy in Bernese mountain dogs. *Vet Pathol* 1994, 31:421–428
  35. Reusch C, Hoerauf A, Lechner J, Kirsch M, Leuterer G, Minkus G, Brem G: A new familial glomerulonephropathy in Bernese mountain dogs. *Vet Rec* 1994, 134:411–415
  36. Center SA, Smith CA, Wilkinson E, Erb HN, Lewis RM: Clinicopatho-logic, renal immunofluorescent, and light microscopic features of glomerulonephritis in the dog: 41 cases (1975–1985). *J Am Vet Med Assoc* 1987, 190:81–90
  37. Cork LC, Morris JM, Olson JL, Krakowka S, Swift AJ, Winkelstein JA: Membranoproliferative glomerulonephritis in dogs with a genetically determined deficiency of the third component of complement. *Clin Immunol Immunopathol* 1991, 60:455–470
  38. Sabnis SG, Gunson DE, Antonovych TT: Some unusual features of mesangioproliferative glomerulonephritis in horses. *Vet Pathol* 1984, 21:574–581
  39. Jansen JH: Porcine membranoproliferative glomerulonephritis with intramembranous dense deposits (porcine dense deposit disease). *APMIS* 1993, 101:281–289
  40. Hogasen K, Jansen JH, Mollnes TE, Hovdenes J, Harboe M: Hered-itary porcine membranoproliferative glomerulonephritis type II is caused by factor H deficiency. *J Clin Invest* 1995, 95:1054–1061
  41. Jansen JH, Hogasen K, Mollnes TE: Extensive complement activation in hereditary porcine membranoproliferative glomerulonephritis type II (porcine dense deposit disease). *Am J Pathol* 1993, 143:1356–1365
  42. Jansen JH, Hogasen K, Harboe M, Hovig T: In situ complement activation in porcine membranoproliferative glomerulonephritis type II. *Kidney Int* 1998, 53:331–349
  43. Maggio-Price L, Russell R, Wolf NS, Alpers CE, Engel D: Clinicopath-ologic features of young and old sph<sup>ha</sup>/sph<sup>ha</sup> mice. Mutants with congenital hemolytic anemia. *Am J Pathol* 1988, 132:461–473
  44. Fulpius T, Berney T, Lemoine R, Pastore Y, Reininger L, Brighthouse G, Izui S: Glomerulopathy induced by IgG3 anti-trinitrophenyl monoclo-nal cryoglobulins derived from non-autoimmune mice. *Kidney Int* 1994, 45:962–971
  45. Fornasieri A, Li M, Armelloni S, de Septis CP, Schiaffino E, Sinico RA, Schmid C, D'Amico G: Glomerulonephritis induced by human IgMK-IgG cryoglobulins in mice. *Lab Invest* 1993, 69:531–540
  46. D'Amico G, Fornasieri A: Cryoglobulinemic glomerulonephritis: a membranoproliferative glomerulonephritis induced by hepatitis C vi-rus. *Am J Kidney Dis* 1995, 25:361–369
  47. Monga G, Mazzucco G, Casanova S, Boero R, Cagnoli L, Barbiano di Belgiojoso G, Confalonieri R: Ultrastructural glomerular findings in cryoglobulinemic glomerulonephritis. *Appl Pathol* 1987, 5:108–115
  48. Stekhoven JH, van Haelst UJ: Unusual findings in the human renal glomerulus in multiple myeloma. A light- and electron-microscopic study. *Virchows Arch B Cell Pathol* 1971, 9:311–321
  49. Bengtsson U, Larsson O, Lindstedt G, Svalander C: Monoclonal IgG cryoglobulinemia with secondary development of glomerulonephritis and nephrotic syndrome. *Q J Med* 1975, 44:491–503
  50. Ogihara T, Saruta T, Saito I, Abe S, Ozawa Y, Kato E, Sakaguchi H: Finger print deposits of the kidney in pure monoclonal IgG kappa cryoglobulinemia. *Clin Nephrol* 1979, 12:186–190
  51. Monga G, Mazzucco G, Coppo R, Piccoli G, Coda R: Glomerular findings in mixed IgG-IgM cryoglobulinemia. Light, electron micro-scopic, immunofluorescence and histochemical correlations. *Vir-chows Arch B Cell Pathol* 1976, 20:185–196
  52. Szymanski IO, Pullman JM, Underwood JM: Electron microscopic and immunochemical studies in a patient with hepatitis C virus infec-tion and mixed cryoglobulinemia type II. *Am J Clin Pathol* 1994, 102:278–283
  53. Feiner H, Gallo G: Ultrastructure in glomerulonephritis associated with cryoglobulinemia. A report of six cases and review of the litera-ture. *Am J Pathol* 1977, 88:145–162
  54. Ahmed SA, Hissong BD, Verthelyi D, Donner K, Becker K, Karpuzo-glu-Sahin E: Gender and risk of autoimmune diseases: possible role of estrogenic compounds. *Environ Health Perspect* 1999, 107(Suppl 5):S681–S686
  55. Ansar Ahmed S, Penhale WJ, Talal N: Sex hormones, immune re-sponses, and autoimmune diseases. Mechanisms of sex hormone ac-tion. *Am J Pathol* 1985, 121:531–551
  56. Verthelyi DI, Ahmed SA: Estrogen increases the number of plasma cells and enhances their autoantibody production in nonautoimmune C57BL/6 mice. *Cell Immunol* 1998, 189:125–134